What Optical Electron-Transfer Reactions Can Teach Us about Electrode Kinetics and Electrocatalysis[1]

Robert L. Blackbourn, Stephen K. Doorn, Jody A. Roberts, and Joseph T. Hupp*

Department of Chemistry, Northwestern University, Evanston, Illinois 60208

Received December 13, 1988. In Final Form: March 9, 1989

A number of ingredients are known or thought to be important in determining rates of electrochemical reactions and, therefore, mechanisms of electrocatalysis. These ingredients may include bond reorganization, solvent reorganization, electronic coupling, ion pairing, proton demand, "work terms", and free-energy driving-force effects. Although evidence exists, in general, for a detectable role for each one of these, for specific cases there is inevitably uncertainty about the relative importance of each effect. Fortunately, optical electron-transfer measurements provide an unambiguous way of partitioning rates into their component effects. The theme of this article is the use of optical processes to learn about molecular level kinetic events and, by inference, molecular level electrocatalysis. We begin by exploring the relationships between electrode processes and analogous optical reactions. Following that, some applications to problems of electrochemical interest—largely drawn from our own recent work—are illustrated. Although the focus is mainly on uncomplicated, single-electron-transfer reactions, preliminary studies of more complicated processes like proton-coupled electron transfer are also mentioned.

Introduction

Electrocatalysis is a pervasive topic in interfacial electrochemistry, and without question electrode kinetics is at the heart of it. In fact, it could reasonably be argued that to the extent that electrode kinetics can be understood in a detailed way (and the accompanying chemistry manipulated) there is the promise of rational and systematic progress in electrocatalysis. With that justification, we note that the traditional approach to understanding both electrocatalysis and electrode kinetics has been to conduct various electrochemical rate studies and to link these to studies of reactant, intermediate, and product adsorption.[2] In favorable cases, the various chemical, electrochemical, and transport steps of complicated reactions can be delineated and the rate-determining steps positively identified.

To proceed further and gain a real molecular or quantum level understanding, additional strategies are required. Perhaps the most common one is to revert to model systems where the key kinetic step (or steps) can be examined in mechanistic isolation. If the key step is interfacial charge transfer, then simple redox reactions are suitable systems. Interfacial redox reactions have, of course, already been investigated extensively.[3] From those investigations (both theoretical[3,4] and experimental[2-4]) has come a broad consensus regarding dynamics and mechanism. Apart from double-layer properties and the effects of adsorption, charge-transfer rates are thought to depend on (1) internal (vibrational) reorganization, (2) thermodynamic driving force (overpotential), and (3) electrode–reactant electronic coupling. A fourth ingredient—solvent reorganization—is widely accepted in other areas of redox chemistry[5] but is considered controversial[6,7] for electrode reactions.

Table I. Information Available from Optical Intervalence Experiments

parameter	information
band energy	classical activation energy
band intensity	site-to-site coupling
band width	sum of vibrational, librational distortions
formal potentials	ground-state energetics, electronic coupling
visible spectrum	extent of bridging ligand mediation
preresonance Raman spectrum	force constants, normal coordinate distortions
spectra in mixed solvents	molecular aspects of solvent reorganization
infrared spectrum	vibrational trapping

Despite this general consensus, there often exists uncertainty or controversy about the relative importance of specific ingredients for any particular reaction.[6] The reason for this may lie in the obvious (but perhaps unwise) reliance upon rates as the primary basis for molecular kinetic investigations. (For example, attempts have been made to derive Franck–Condon barriers from slopes of Arrhenius rate plots, tunneling and electronic factors from their intercepts, solvent reorganizational barriers from rate measurements as a function of medium, and so on.) The difficulty here is that rates can respond simultaneously to a myriad of kinetic and molecular factors. For example, solvent effects on redox rates have variously been attributed to dynamical effects,[8] ion-pairing effects,[9,10] adsorption phenomena,[11] hydrogen-bonding effects (ligand to solvent),[12] electronic coupling,[13] and internal-mode variations,[12] in addition to the expected classical variation in the electrostatic barrier to solvent reorganization.[4] It may be unreasonable, then, to expect (routinely, at least) to gain accurate, detailed information about any single factor solely from electrochemical rate measurements.

(1) Presented at the symposium entitled "Electrocatalysis", 196th National Meeting of the American Chemical Society, Los Angeles, CA, Sept 27-29, 1988.

(2) See, for example: *Chemistry and Physics of Electrocatalysis*; McIntyre, J. D. E., Weaver, M. J., Yeager, E., Eds.; Electrochemical Society: Pennington, NJ, 1984.

(3) For a recent review, see: Weaver, M. J. In *Comprehensive Chemical Kinetics*; Compton, R. G., Ed.; Elsevier: Amsterdam, 1988; Vol. 27.

(4) Marcus, R. A. *J. Chem. Phys.* **1965**, *43*, 679.

(5) Cannon, R. D. *Electron Transfer Reactions*; Butterworths: London, 1980.

(6) Bockris, J. O.'M.; Kahn, S. U. M. *Quantum Electrochemistry*; Plenum Press: New York, 1979.

(7) (a) Kahn, S. U. M.; Bockris, J. O.'M. in ref. 2. (b) Kahn, S. U. M.; Bockris, J. O.'M. *J. Phys. Chem.* **1983**, *87*, 4012. (c) Kahn, S. U. M.; Bockris, J. O.'M. *Chem. Phys. Lett.* **1983**, *99*, 83. (d) Bockris, J. O.'M.; Sen, R. K. *Mol. Phys.* **1975**, *29*, 357.

(8) Representative electrochemical references: (a) Kapturkiewicz, A.; Behr, B. *J. Electroanal. Chem.* **1984**, *174*, 187. (b) Gennett, T.; Weaver, M. J. *Chem. Phys. Lett.* **1985**, *113*, 213. (c) Gennett, T.; Milner, D.; Weaver, M. J. *J. Phys. Chem.* **1985**, *89*, 2787. (d) Zhang, X.; Leddy, J.; Bard, A. J. *J. Am. Chem. Soc.* **1985**, *107*, 3719.

(9) Blackbourn, R. L.; Hupp, J. T. *J. Phys. Chem.*, submitted.

(10) Borchardt, D.; Wherland, S. *Inorg. Chem.* **1984**, *23*, 2537.

(11) Farmer, J. K.; Gennett, T.; Weaver, M. J. *J. Electroanal. Chem.* **1985**, *191*, 357.

(12) (a) Chang, J. P.; Fung, E. Y.; Curtis, J. C. *Inorg. Chem.* **1986**, *25*, 4233. (b) Curtis, J. C.; Sullivan, B. P.; Meyer, T. *J. Inorg. Chem.* **1983**, *22*, 224. (c) Lay, P. A. *J. Phys. Chem.* **1986**, *90*, 878. (d) Hupp, J. T.; Weaver, M. J. *J. Phys. Chem.* **1985**, *89*, 1601. (e) Fung, E. Y.; Chua, A.; Curtis, J. C. *Inorg. Chem.* **1988**, *27*, 1294.

(13) Hupp, J. T. *J. Am. Chem. Soc.*, submitted.

0743-7463/89/2405-0696$01.50/0

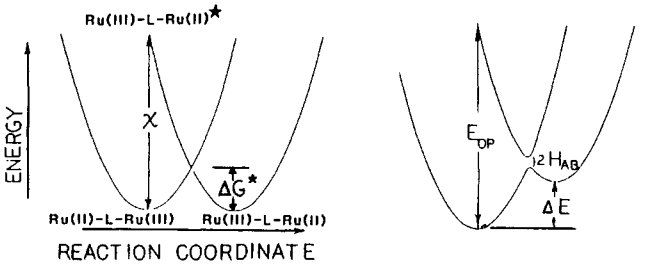

Figure 1. Schematic representation of energy relationships for optical and thermal electron transfer in symmetrical and unsymmetrical mixed-valence systems.

What is needed, in our opinion, are independent probes and measurements of those parameters or effects believed to contribute to the kinetics of electrochemical reactions. A spectacular example of what we mean is the implimentation of solution EXAFS in electrochemical systems.[14,15] This technique has justifiably achieved wide acclaim because it can yield in situ bond length changes (and, therefore, vibrational barriers) for selected redox systems.[16]

Another example, admittedly much less well-known (at least in electrochemical situations), is the use of optical electron-transfer (ET) reactions as redox probes.[17] As noted in Table I, this approach can also yield bond length information.[18] Furthermore, it can give information about solvent reorganization, electronic interactions, and various environmental perturbations.[17,19] The key point from the table (and the following discussion) is that the information is generated in a way that largely decouples the parameters from each other and from the uncertainties of rate theory.

The theme of the remainder of this article is the use of optical processes to learn about molecular level kinetic events and, by inference, molecular level electrocatalysis. We begin in the next section by exploring the relationships between electrode processes and analogous optical reactions. Following that, some applications to problems of electrochemical interest—largely drawn from our own recent work—are illustrated. Although the focus is mainly on uncomplicated, single-electron-transfer reactions, preliminary studies of EC processes like proton-coupled electron transfer are also mentioned.[68]

Relationships between Optical and Electrochemical Events and a Primer on Optical Electron-Transfer Reactions

Equation 1 shows a prototypical example of an optical electron-transfer reaction.

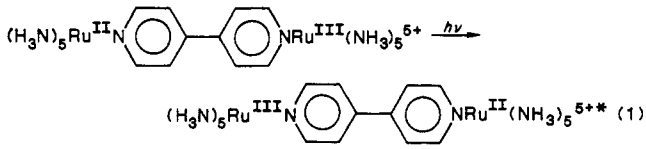

(1)

In the reaction, metal-to-metal (or "intervalence") charge transfer occurs between coordinatively identical redox sites which are bridged by a symmetrical organic ligand. A schematic representation of the energetics is shown in Figure 1.

From Figure 1 and eq 1, some analogies to electrode processes should be readily apparent (for example): (1) The intervalence reaction involves back-to-back anodic and cathodic processes but with an organic bridge in place of an electrode as an electron-transfer mediator. (2) In the symmetrical mixed-valence case (i.e., eq 1), ΔG is zero and the intervalence reaction is most nearly likened to an electrochemical exchange process occurring at the redox formal potential. On the other hand, when the reaction is unsymmetrical there exists a thermodynamic driving force which is analogous to an overpotential. (3) In the optical reaction, the kinetic barrier to charge transfer is overcome by absorption of a photon; in the electrochemical reaction, it is instead surmounted by thermal activation. (It should be noted, however, that a "dark" pathway (thermally activated) exists for the mixed-valence complex as well.)

Further interpretation of Figure 1 suggests how one might extract kinetically useful information from the optical experiment. In the figure, the optical event is sketched as a vertical transition because, in a classical sense, light absorption occurs on a time scale that is short compared with nuclear motion (i.e., the nuclear coordinates effectively are frozen). On the other hand, in a quantum or spectroscopic sense the process is "vertical" because this allows for maximum overlap between ground-state (mostly $v = 0$) and excited-state vibrational wave functions.[20] There are, of course, finite overlaps (or "Franck–Condon factors") for an energetic range of nonvertical transitions, and these help to provide breadth to the optical absorption band.[20]

In either picture, the optical transition leads to a product state that exists initially in a vibrationally excited form. As suggested by Figure 1, the energy of the absorbed photon provides a direct measure of the cost of creating this vibrationally excited form and also provides a one-point "mapping" of the product location.[19] In the absence of complications, a second point along the energy axis (i.e., the product's zero point energy) is defined by the symmetry of the reaction (or in an unsymmetrical case by the state-to-state redox asymmetry if that quantity is independently established—for example, by electrochemistry). In principle, the remaining points can be mapped by deconvoluting the entire absorption band. In practice, what is generally done is to assume symmetrical, parabolic potential energy surfaces. (In the case of eq 1, symmetry, at least, is assured by the symmetry of the optical reaction.) It follows then that the intersection point of the curves (corresponding to the classical activation energy ΔG^*) occurs at just one-fourth the optical barrier height; for the analogous electrochemical reaction, ΔG_e^* (or at least its vibrational component) will be *one-eighth* that in the optical reaction.

The optical barrier height itself is given by the energy (E_{op}) at the intervalence absorption maximum. More generally, if electronic asymmetry (ΔE) exists (i.e., if the wells of the curves in Figure 1 are vertically displaced), ΔG^* is given by[19]

$$\Delta G^* = (E_{op} - \Delta E)/4 \quad (2)$$

It should be noted that the optical experiment and eq 2

(14) (a) Dewald, H. D.; Watkins, J. W.; Elder, R. C.; Heineman, W. R. *Anal. Chem.* **1986**, *58*, 2968. (b) Blum, L.; Abruña, H. D.; White, J.; Gordon, J. G., II; Borges, G. L.; Samant, M. G.; Melroy, O. R. *J. Chem. Phys.* **1986**, *85*, 6732.

(15) Another important example (or family of examples) is the application of surface science techniques to emersed electrochemical systems. These techniques can directly yield *interfacial* structural information about reactive systems. An extensive review has been written recently by Hubbard (*Chem. Rev.* **1988**, *88*, 633).

(16) Much of the available data for transition-metal redox systems is collected in: Brunschwig, B. S.; Creutz, C.; Macartney, D. H.; Sham, T.-K.; Sutin, N. *Faraday Discuss.* **1982**, *74*, 113.

(17) For a recent review, see: Creutz, C. *Prog. Inorg. Chem.* **1983**, *30*, 1.

(18) (a) Doorn, S. K.; Hupp, J. T. *J. Am. Chem. Soc.* **1989**, *111*, 1142. (b) Doorn, S. K.; Hupp, J. T. *J. Am. Chem. Soc.*, in press.

(19) (a) Hush, N. S. *Prog. Inorg. Chem.* **1967**, *8*, 391. (b) Hush, N. S. *Trans. Faraday Soc.* **1961**, *57*, 557.

(20) An instructive discussion can be found in Schwartz, S. E. *J. Chem. Ed.* **1973**, *50*, 608.

Table II. Analogies between Kinetic Parameters for Electrode Reactions and Optical Parameters for Intervalence Transitions

electrochemical reaction	optical transition
adiabaticity	oscillator strength
solvent reorganization	line shape and transition energy
bond reorganization	intervalence-enhanced Raman scattering intensities
overpotential	redox asymmetry
environmental effects (electrolyte, mixed solvation, reactant aggregation, etc.)	optical and spectroscopic perturbations

provide a "direct" route (i.e., nonkinetic) to ΔG^* that is independent of assumptions regarding activated complex theory, the existence of transition states, and so on.

As we shall see in the following section, it is possible with more elaborate experiments to obtain considerably more information than simply the overall size of the barrier. In particular, one can separate the role of solvent from that of vibrational reorganization. Furthermore, the vibrational part can be separated in a detailed way into component normal-mode distortions by using recently developed Raman techniques.[18,21] Table II draws some further analogies between electrochemical and optical parameters.

One other issue that merits discussion in this background section is the general question of nonadiabaticity[22] and the role of electronic interactions between the electrode surface and the appropriate donor or acceptor orbital of the reactant. Theorists usually express these interactions in terms of coupling between initial and final states (where the initial state represents, for example, the state with the electron on the solution donor and the final state is the one consisting of an oxidized donor and an extra electron in the electrode's conduction band, or vice versa). The reason this is important is that if the coupling is weak enough (in other words, if the initial state/final state matrix element $\bar{H}_{13}$ is small enough),[23] then the first-order rate (s^{-1}) for electron transfer to the electrode from the reactant, when the reactant is located in an appropriate precursor state, is equal to the square of the matrix element multiplied by the Franck–Condon weighted (and Boltzmann weighted) density of states. For our purposes, the latter is reasonably approximated by $\exp(-\Delta G^*/RT)$. This relationship between coupling and rate is simply Fermi's golden rule[24] and should apply whenever we are in the so-called nonadiabatic limit. Physically this limit describes the case in which the radiationless electronic transition itself (rather than internal-coordinate or solvent motion) provides the rate-limiting dynamics.

The evaluation of $\bar{H}_{13}$ for electrochemical reactions is a challenging task. It turns out to be appreciably easier, however, for analogous optical events. For weak intervalence transfer, $\bar{H}_{13}$ can be estimated directly from E_{op} and the integrated intensity of the absorption band.[19] The

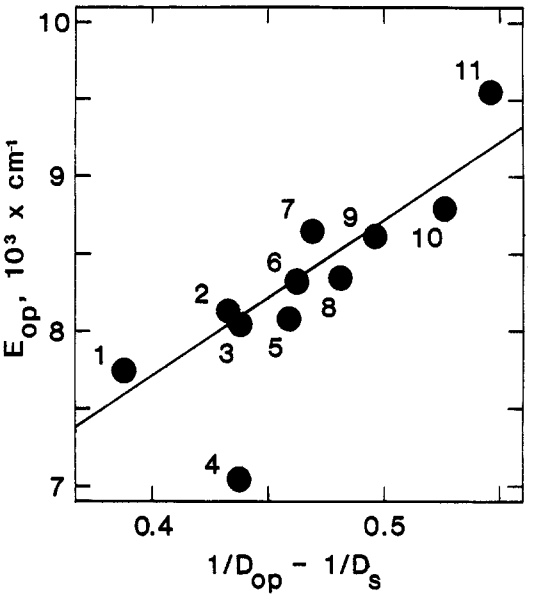

Figure 2. Intervalence transfer band energies vs $1/D_{op} - 1/D_s$. Key to solvents: (1) nitrobenzene, (2) dimethyl sulfoxide, (3) 1-methyl-2-pyrrolidone, (4) hexamethylphosphoramide, (5) dimethylacetamide, (6) dimethylformamide, (7) formamide, (8) propylene carbonate, (9) acetone, (10) acetonitrile, and (11) deuterium oxide.

precision with which such mesurements can be made enables the effects of distance, intervening orbital composition, and thermodynamic driving force to be evaluated in a quantitative fashion.[17,25]

Applications

Solvent Reorganization. One of the more contentious points[6,7] in electrode kinetics is the question of how—or even if—the solvent contributes to the definition of the initial- and final-state potential energy surfaces and therefore to the activation free energy for interfacial charge transfer. According to Marcus,[4] the occurrence of "nonequilibrium solvent polarization" in polar solvents should lead to an electrochemical activation energy contribution $\Delta G_{e,o}^*$ of the form

$$\Delta G_{e,o}^* = \frac{e^2}{8}\left(\frac{1}{r} - \frac{1}{R}\right)\left(\frac{1}{D_{op}} - \frac{1}{D_s}\right) \qquad (3)$$

In eq 3, e is the unit electronic charge, r is the reactant radius, R is the distance between the transition state and its image charge in the electrode, D_{op} is the solvent's optical dielectric constant (i.e., the square of the refractive index), and D_s is the solvent's static dielectric constant. As we have noted in the Introduction, various attempts either to prove or disprove eq 3 have, for a variety of reasons, met with little success, and the ultimate conclusions have been less than convincing.

For optical ET, there exists an entirely analogous formulation:[19]

$$\Delta G_{e,o}^* = \chi_s/4 = \frac{e^2}{4}\left(\frac{1}{r} - \frac{1}{d}\right)\left(\frac{1}{D_{op}} - \frac{1}{D_s}\right) \qquad (4)$$

In eq 4, χ_s is the solvent reorganization energy and d is the site-to-site separation distance. We can also write[19]

$$E_{op} = \chi_s + \chi_i + \Delta E + \Delta E' \qquad (5)$$

(21) (a) Heller, E. J.; Sundberg, R. L.; Tannor, D. *J. Phys. Chem.* **1982**, *86*, 1822. (b) Tannor, D.; Heller, E. J. *J. Chem. Phys.* **1982**, *77*, 202. (c) Lee, S. Y.; Heller, E. J. *J. Chem. Phys.* **1977**, *71*, 4777. (d) Heller, E. J. *Acc. Chem. Res.* **1981**, *14*, 368.

(22) For a concise discussion of nonadiabatic rate formulations for homogeneous electron-transfer reactions, see: Brunschwig, B. S.; Sutin, N. *Comm. Inorg. Chem.* **1987**, *6*, 209.

(23) The notation $\bar{H}_{13}$ is from Marcus (*Chem. Phys. Lett.* **1987**, *133*, 471; **1988**, *146*, 13) and is used in anticipation of a role for a bridge or other intervening medium (designated as site 2 by Marcus) in facilitating charge transfer.

(24) Atkins, P. W. *Molecular Quantum Mechanics*, 2nd ed., Oxford University Press: Oxford, 1983.

(25) (a) Richardson, D. E.; Taube, H. *J. Am. Chem. Soc.* **1983**, *105*, 40. (b) Richardson, D. E.; Taube, H. *Coord. Chem. Rev.* **1984**, *60*, 107.

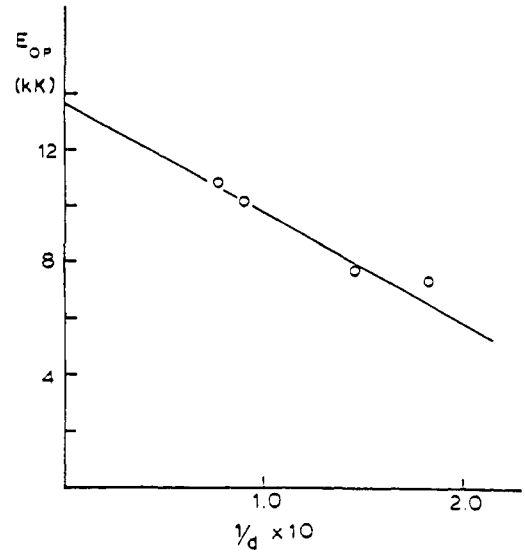

Figure 3. Plot of E_{op} vs $1/d$ for the mixed-valence dimers $[(bpy)_2ClRu(L)RuCl(bpy)_2]^{3+}$ (L = pyrimidine (pym), pyrazine (pyr), 4,4'-bipyridine (4,4'-bpy), *trans*-1,2-bis(4-pyridyl)ethylene (BPE)) in acetonitrile (from ref 29).

where χ_i is the inner-shell or vibrational reorganization energy, ΔE is the redox asymmetry, and $\Delta E'$ accounts for any additional energetic effects due to intervalence transfer to an electronic excited state. (Such effects turn out to be fairly common for second- and third-row transition-metal dimers on account of $d\pi$ orbital splittings induced by spin–orbit coupling.[17,26,27])

The combination of eq 4 and 5 suggests a number of simple tests based on E_{op} measurements. Figure 2 shows a test where E_{op} for eq 1 has been plotted versus the solvent parameter $(1/D_{op} - 1/D_s)$.[29] A correlation indeed exists, and the result has been corroborated for other systems.[17,28-30] Figure 3 shows a related test from a study by Meyer and co-workers.[29,30] For the bridging ligands pyrimidine ($d \approx 6$ Å), pyrazine ($d = 6.9$ Å), 4,4'-bipyridine ($d = 11.3$ Å), and bis(pyridyl)ethylene ($d = 14.3$ Å), they examined the dependence of E_{op} on separation distance and found the inverse dependence predicted by eq 4.

Tests of this kind indicate very clearly that solvent reorganization is a requirement for optical charge transfer. Furthermore, the Marcus–Hush dielectric continuum description[4,19] appears, qualitatively at least, to be correct. (Quantitative aspects have been discussed at length by Brunschwig, Ehrenson, and Sutin.[31]) Nevertheless, the experiments and theoretical descriptions lead only to a macroscopic understanding of nonequilibrium solvent polarization.

We have recently described a series of experiments designed instead to probe *molecular* aspects of solvent reorganization.[32] The question we specifically wanted to answer was, which molecules—and how many—are involved in solvent reorganization? The experiments that were devised were based on molecular level radial segregation of the solvent around particular metal complexes. Chemically, the segregation was achieved by hydrogen bonding a monolayer of a strongly donating solvent (dimethyl sulfoxide, DMSO) to the "ammine surface" of a strongly accepting complex: $(H_3N)_5Ru^{II}$–(4,4'-bpy)$Ru^{III}(NH_3)_5^{5+}$. When DMSO is present only as a minority component, the composition in the second solvation layer and beyond is largely that of the majority solvent, CH_3CN.

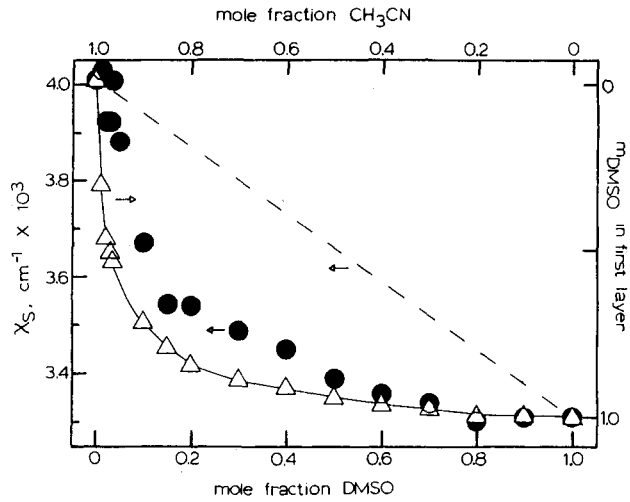

Figure 4. Dependence on bulk solvent composition: (●) χ_s for optical electron transfer in $[(NH_3)_5Ru^{II}$–4,4'-bpy–$Ru^{III}(NH_3)_5]^{5+}$; (△) first solvation layer composition (see text). Dashed line corresponds to a hypothetical linear relationship between χ_s and bulk solvent composition.

The key question is whether χ_s reflects primarily the first-layer composition or, instead, longer range phenomena. The answer is contained, in part, in Figure 4. In the figure, the composition of the first solvation layer about the dimer is shown to depend strongly on the bulk solvent composition for mole fractions of DMSO (m_{DMSO}) less than about 0.2. In other words, only a minor fraction of DMSO is required in the bulk in order to encase the complex locally in that solvent. Also shown is a dashed diagonal line which would represent a hypothetical linear relationship between χ_s and bulk solvent composition. Finally, the actual experimental dependence of χ_s is shown by the filled circles. From the figure, the most important observation is that χ_s comes close to matching the dependence of the first-layer composition on bulk solvent composition. Evidently, most of the solvent reorganization energy (ca. 80%) comes from first-layer polarization.

From mixed-solvent NMR studies[33] for the related ion $Cr(NH_3)_5DMSO^{3+}$, it has been argued that this first layer will contain (for the dimer) a total of about 20 solvent molecules. The significance of this is twofold: (1) it suggests that the overall problem is physically small enough that detailed and accurate molecular level modeling will eventually be possible;[34] (2) it negates one of the persistent objections[6,7d] to the theory of nonequilibrium solvent polarization, namely, that the simultaneous activation of several hundred (or thousand) solvent molecules is a statistically unlikely occurrence. (Simultaneous activation of a large number of molecules was thought to be implicit in the theory, based on comments by Levich.[35])

(26) Hupp, J. T.; Meyer, T. J. *Inorg. Chem.* **1987**, *26*, 2332.
(27) Kober, E. M.; Goldsby, K. A.; Narayana, D. N. S.; Meyer, T. J. *J. Am. Chem. Soc.* **1985**, *105*, 4303.
(28) Representative references: (a) Tom, G. M.; Creutz, C.; Taube, H. *J. Am. Chem. Soc.* **1974**, *96*, 7828. (b) Sullivan B. P.; Meyer, T. J. *Inorg. Chem.* **1980**, *19*, 752. (c) Sullivan, B. P.; Curtis, J. C.; Kober, E. M.; Meyer, T. J. *Nouv. J. Chem.* **1980**, *4*, 643. (d) Amer, S. I.; Dasgupta, T. P.; Henry, P. M. *Inorg. Chem.* **1983**, *22*, 1970. (e) Palaniappan, V.; Agarwala, U. C. *Inorg. Chem.* **1988**, *20*, 3568.
(29) Powers, M. J.; Meyer, T. J. *J. Am. Chem. Soc.* **1980**, *102*, 1289.
(30) See also: Powers, M. J.; Meyer, T. J. *J. Am. Chem. Soc.* **1978**, *100*, 4393.
(31) Brunschwig, B. S.; Ehrenson, S.; Sutin, N. *J. Phys. Chem.* **1986**, *90*, 3657; **1987**, *91*, 4714.
(32) Blackbourn, R. L.; Hupp, J. T. *J. Phys. Chem.* **1988**, *92*, 2817.
(33) Reynolds, W. L.; Reichley-Yinger, L.; Yayn, Y. *Inorg. Chem.* **1985**, *24*, 4273.
(34) This conclusion is reinforced by recent Monte-Carlo calculations: Hatano, Y.; Saito, M.; Kakitani, T.; Mataga, N. *J. Phys. Chem.* **1988**, *92*, 1008.

Admittedly, none of these observations "proves" that solvent reorganization also occurs in electrode reactions. Nevertheless, the conceptual similarity between the optical and electrochemical processes suggests, at the very least, that it would be prudent to take solvent barrier effects into consideration when attempting to interpret the kinetics of simple electrode reactions.

Reactivity in Mixed Solvents. One of the unexpected bonuses of our study of solvent reorganization has been the opportunity to monitor some unusual (and kinetically significant) barrier effects which evidently are unique to mixed solvents.[36,37] Figure 5 shows an example of what we have in mind. For the intervalence reaction in eq 1 in mixtures of CH_3CN + DMSO as solvent, the directly measured optical barrier to charge transfer (E_{op}) shows a very peculiar dependence on solvent. E_{op} is marked by a very sharp rise ($\Delta E_{op} \approx 1100\ cm^{-1}$) and then a more gradual decline with addition of DMSO to acetonitrile as solvent. A detailed investigation enabled us to rule out the more obvious possibilities for this behavior (e.g., solute degradation, grossly nonlinear dielectric characteristics, etc.). Eventually, it was found that the effect was due to *unsymmetrical* selective solvation by DMSO. In other words, selective solvation was shown to exist for both $(NH_3)_5Ru^{III}$ and $(NH_3)_5Ru^{II}$ but was found to be appreciably more substantial for the fragment in the higher oxidation state.

Equation 6 illustrates the consequences of this unsymmetrical solvation, following optical excitation. In the charge-transfer excited state, $(NH_3)_5Ru^{II}$ finds itself in a solvent environment appropriate to $(NH_3)_5Ru^{III}$, and the reverse is true at the other end. The increase in E_{op}, then, is simply a measure of how expensive it is to create these mismatched solvent environments. At the energy peak in Figure 5, excited-state relaxation requires either back electron transfer or the *net* translation of about five DMSO molecules from $(NH_3)_5Ru^{III}$ to $(NH_3)_5Ru^{II}$. To an electrochemist, the latter possibility would be immediately recognizable as an optical EC reaction—the C step being solvent translation.

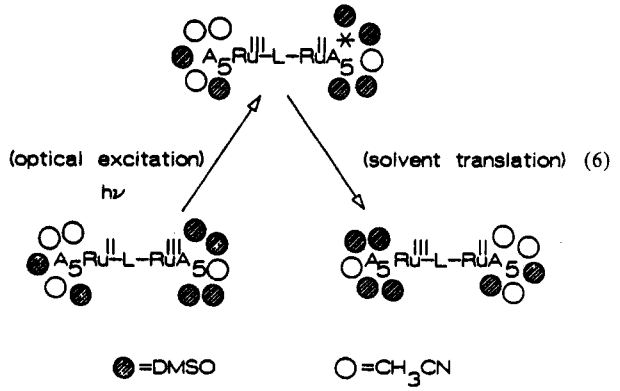

Given that analysis, the optical energetics can be understood largely in terms of vertical displacements of the initial- and final-state surfaces in Figure 1 (see also Figure 12). (Residual horizontal displacements are essentially what is described by the changes in χ_s in Figure 4; that figure was generated by correcting Figure 5 for the energy due to unsymmetrical solvation.[32]) These vertical displacements lead to a corresponding displacement in the curve–intersection region. If the displacement is not too severe, then the expected relationship is $0.5\Delta E_{op} \approx \Delta\Delta G^*$. Note that an increase in ΔG^* implies an exponential decrease in rate for the corresponding thermal ET reaction.

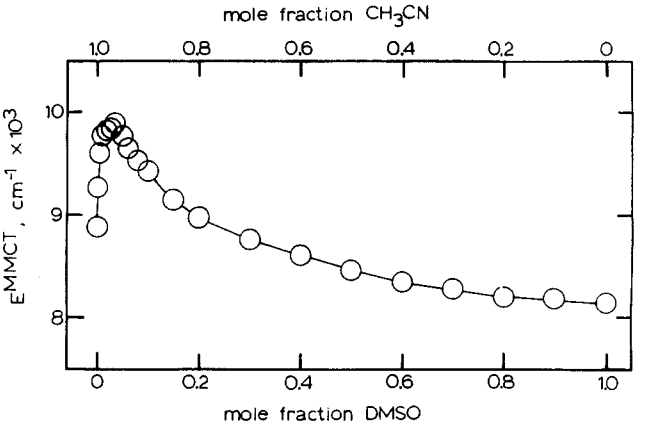

Figure 5. Dependence of E_{op} for metal-to-metal charge transfer in $[(NH_3)_5Ru^{II}$-4,4′-bpy-$Ru^{III}(NH_3)_5]^{5+}$ on solvent composition in acetonitrile/DMSO mixtures.

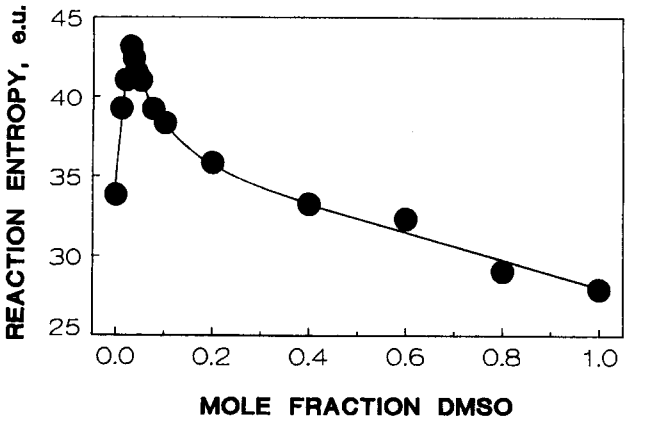

Figure 6. $\Delta S_{rc}°$ vs solvent composition for reduction of $(NH_3)_5Ru(py)^{3+}$ in mixtures of CH_3CN + DMSO.

The lesson we have taken from this is that similar effects ought to exist for related electrochemical reactions, e.g.:

$$(1-x)CH_3CN,\ x\,DMSO\left[(NH_3)_5Ru^{III}N\bigcirc\right]^{3+} + e^- \xrightarrow{E}$$

$$(1-x)CH_3CN,\ x\,DMSO\left[(NH_3)_5Ru^{II}N\bigcirc\right]^{2+} \xrightarrow{C}$$

$$(1-y)CH_3CN,\ y\,DMSO\left[(NH_3)_5Ru^{II}N\bigcirc\right]^{2+} + (y-x)CH_3CN \quad (7)$$
$$+$$
$$(x-y)\,DMSO$$

In eq 7, x, y, $1-x$, and $1-y$ signify fractional occupancies of the second sphere. Furthermore, one should be able to map (and predict) the effects optically.

Unfortunately, the mixed-solvent kinetics of reactions like eq 7 have not been reported. However, two points are worth noting. First, thermodynamic reaction entropy measurements, specifically for the reaction in eq 7, corroborate the idea of redox-induced solvation layer rearrangement. As shown by Figure 6, there exists a "spike" in a plot of reaction entropy versus solvent composition. The important point is that the spike occurs in precisely the region where entropy generation from release of DMSO is anticipated to be most significant. Elsewhere, this point is elaborated, and some additional implications are presented.[38]

(35) Levich, V. G. In *Physical Chemistry: An Advanced Treatise*; Eyring, H., Henderson, D., Jost, W., Academic Press: New York, 1980; Vol. IXB, p 1006.
(36) Hupp, J. T.; Weydert, J. *Inorg. Chem.* **1987**, *26*, 2657.
(37) See also: Ennix, K. S.; McMahon, P. T.; Curtis, J. C. *Inorg. Chem.* **1987**, *26*, 2660.

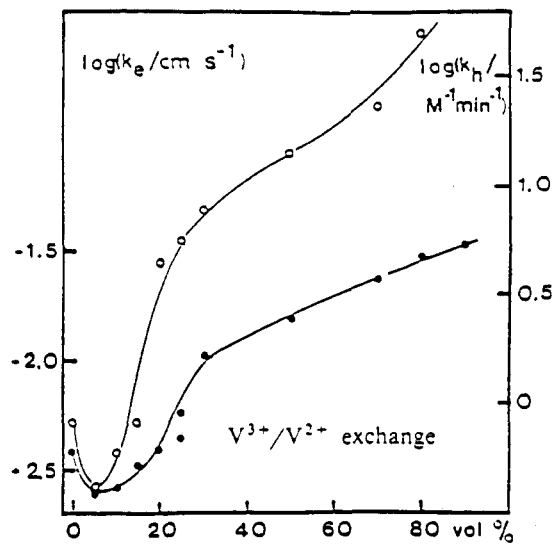

Figure 7. Plot of the logarithm of homogeneous (○) and electrochemical (●) electron-exchange rate constants for $V^{3+/2+}$ against vol % of DMF in mixtures of dimethylformamide + water as solvent (from ref 39a).

The second point is that there are in fact numerous reports of mixed-solvent kinetics—both for homogeneous and heterogeneous ET reactions. In a surprisingly large number of these, rate decreases occur upon addition of a small amount of a second solvent.[39] Typically the rate recovers, however, with further additions. An example from a report by Lipkowski and co-workers[39a] is shown in Figure 7. We suggest that observations like the ones in Figure 7 are manifestations of the EC nature of these reactions (see above) and that they may be interpreted in much the same way as the optical reactions.[40]

Vibrational Barriers in Charge-Transfer Reactions. It is well-known from radiationless decay theory[41] and from classical ET theory[4,19] that whenever a vibrational frequency change or mode distortion accompanies an oxidation-state change a vibrational (Franck–Condon) barrier will be created for that transition. In terms of local coordinates, this boils down to changes in force constants and in lengths of bonds. In many cases, these effects can provide the largest fraction of the intrinsic activation barrier to an electrode (or homogeneous) reaction. Thus, a quantitative knowledge of the extent of their occurrence is virtually a necessity for a complete interpretation of the rate of the reaction.

We have recently begun to develop an approach which can yield precisely the desired information. The methodology is based on the observation of intervalence-enhanced Raman scattering.[18]

(38) Blackbourn, R. L.; Hupp, J. T. *Inorg. Chem.*, submitted.
(39) Representative references: (a) Wilson, J.; Hwa Tai Ting, O.; Lipkowski, J. *J. Electroanal. Chem.* **1988**, *247*, 85. (b) Hotan, Z. C.; Amis, E. S. *J. Inorg. Nucl. Chem.* **1966**, *28*, 2899. (c) Vicenti, M.; Pramauro, E.; Pelizetti, E. *Transition Met. Chem.* **1985**, *8*, 273. (d) Mayhew, R. T.; Amis, E. S. *J. Phys. Chem.* **1975**, *79*, 862. (e) Micic, O. I.; Cercek, B. *J. Phys. Chem.* **1974**, *78*, 285. (f) Micic, O. I.; Cercek, B. *J. Phys. Chem.* **1977**, *81*, 833. (g) Holba, V.; Harcarova, V.; Tarnovska, M. *Chem. Zvesti* **1983**, *37*, 721. (h) Cetnanska, M.; Stroka, J. *J. Electroanal. Chem.* **1987**, *234*, 263. (i) Broda, J.; Galus, Z. *J. Electroanal. Chem.* **1983**, *145*, 147. (j) Maksymiuk, K.; Stroka, J.; Galus, Z. *J. Electroanal. Chem.* **1987**, *226*, 315. (k) Gorski, W.; Galus, Z. *J. Electroanal. Chem.* **1987**, *237*, 209. (l) Jaenicke, W.; Schweitzer, P. H. *Z. Phys. Chem. (N.F.)* **1967**, *52*, 104. (m) Bregler, T.; Gonzales, E. R.; Parson, R. *Collect. Czech. Chem. Commun.* **1971**, *36*, 414.
(40) An important difference in many of the electrochemical reactions (including the one in Figure 7) is that these involve changes not only in second-sphere but also in first-sphere coordination.
(41) Jortner, J. *Philos. Mag.* **1979**, *40*, 317.

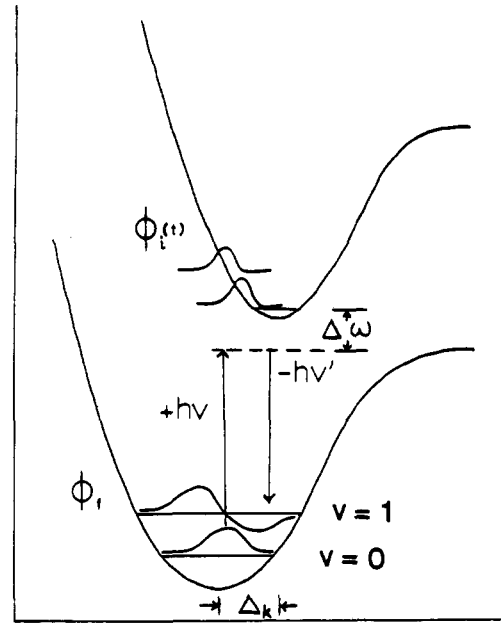

Figure 8. Schematic depiction of the semiclassical analysis of Raman scattering. $\Delta\omega$ is the energy mismatch between the excitation source and the excited-state potential surface. $\phi_i(t)$ is the initial wave packet propagated in time on the excited-state surface. Its time-dependent overlap with ϕ_f, the final vibrationally excited state of the ground electronic surface, defines the Raman polarizability.

The underlying theory comes from work by Heller and co-workers.[21] They have shown that a versatile theoretical approach to Raman scattering problems—especially those involving resonance enhancement—is one based on wave-packet propagation. Raman excitation at or near resonance leads, in this picture, to the projection of a wave packet onto an excited-state potential energy surface. The evolution of this wave packet in the time domain leads to a time-dependent overlap with a vibrational wave function on the ground electronic surface (see Figure 8). In the limit of "short time dynamics" (achieved experimentally at pre- or postresonance), the magnitude of the overlap at a specified time, for a specified mode, depends on the relative steepness of the upper potential energy surface and its "horizontal" displacement from the lower one. This is important because the extent of overlap defines the Raman polarizability, which in turn defines the intensity for electronically enhanced Raman scattering.

Since, for any particular mode, the surface steepness and upper/lower horizontal displacement define, respectively, the vibrational force constant and unitless coordinate displacement (Δ), there is an opportunity to extract these important quantities from relative Raman intensity (I) measurements under conditions of modest resonance enhancement. In the simplest case, Heller and co-workers write[21]

$$\frac{I_1}{I_2} = \frac{\omega_1^2\Delta_1^2}{\omega_2^2\Delta_2^2} \tag{8}$$

$$2\sigma^2 = \sum_k \Delta_k^2(\omega_k/2\pi)^2 \tag{9}$$

where ω is 2π times the vibrational frequency (ν) and $8\sigma^2$ is the square of the absorption bandwidth at $1/e$ of the height. If a local coordinate approximation is appropriate, the Δ values from eq 8 and 9 can be converted to absolute bond distortions ($|\Delta a|$) by

$$|\Delta a| = (\Delta^2\hbar/\mu\omega b)^{1/2} \tag{10}$$

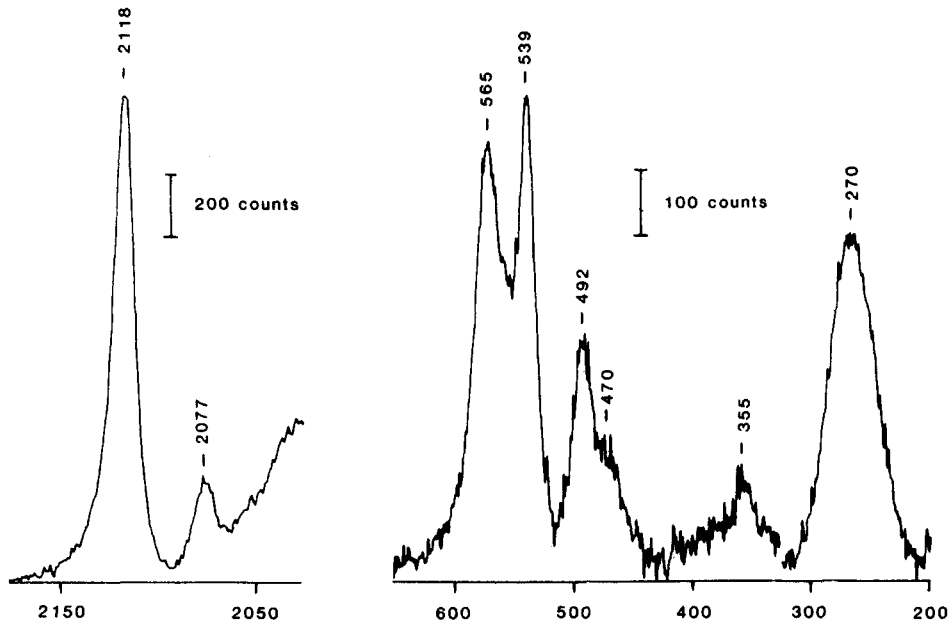

Figure 9. Postresonance Raman spectrum of 40 mM $(CN)_5Ru-CN-Ru(NH_3)_5^{1-}$ in H_2O with 514.5-nm excitation.

where μ is the reduced mass and b is the effective bond degeneracy. Finally, from classical electron-transfer theory the intrinsic vibrational activation energy is given by

$$4\Delta G_i^* = \tfrac{1}{2}\sum fb(\Delta a)^2 = \chi_i \qquad (11)$$

where the force constant f equals $4\pi^2\nu^2c^2\mu^2$ and c is the velocity of light.

To illustrate the approach, we will consider the optical electron-transfer reaction occurring within the unsymmetrical dimer $(NC)_5Ru^{II}-CN-Ru^{III}(NH_3)_5^{1-}$ (1):

$$(NC)_5Ru^{II}-CN-Ru^{III}(NH_3)_5^{1-} \xrightarrow{h\nu} (NC)_5Ru^{III}-CN-Ru^{II}(NH_3)_5^{1-*} \qquad (12)$$

In 1, an intervalence absorption band of moderate intensity exists with λ_{max} = 684 nm in water.[42] Laser excitation at postresonance (514.5 nm) leads to enhanced Raman scattering, as shown in Figure 9. The key feature of the spectrum is that *enhanced scattering is observed from both ends of the mixed-valence ion, based on a single electronic excitation.* For example, an ammine–Ru stretch occurs at 492 cm^{-1}, and C≡N stretches exist at 2077 (weak) and 2118 cm^{-1} (strong). The shift of the strong band to a higher energy than found for free $[Ru(CN)_6]^{4-}$,[43] in addition to the observation of greater effects of solution acidity upon the weak band, lead us to assign the 2118-cm^{-1} mode as the bridging CN stretch.[44] The weak band is then assigned as the terminal CN stretch.

Additional bands exist at 565 and 539 cm^{-1}, corresponding to a single band assigned as the ν_7 mode in hexacyano metal monomers.[43] This mode has been shown to contain both M–CN stretching and M—C≡N bending character.[45] On the basis of the shift to lower energy from that found for the monomer, the band at 539 cm^{-1} is assigned as a distortion associated with the bridge and the higher energy band as a terminal M–CN distortion.[46] The bands at 270 and 470 cm^{-1} shift to lower energy upon ammine deuteration and are assigned as an $H_3N-Ru-NH_3$ bend[17] and an additional Ru–NH_3 stretch, respectively. The band at 355 cm^{-1} is tentatively assigned as the Ru–NC stretch.

Analysis of the scattering intensities using eq 8–10 leads to the structural parameters listed in Table III. The values obtained are reasonably consistent with the few available direct structural assessments for related systems: (1) For $Ru(NH_3)_6^{3+/2+}$, the metal–ammonia bond length change is 0.04 Å by X-ray crystal structure measurements[16] versus 0.039 Å from Raman measurements with the mixed-valence ion. (2) For $Fe(CN)_6^{3-/4-}$, Δa_{M-C} is −0.026 Å[47] versus ±0.035 Å in 1,[48,49] if the ν_7 mode is attributed com-

Table III. Structural and Franck–Condon Charge-Transfer Parameters for $(NC)_5Ru-CN-Ru(NH_3)_5^-$ from Postresonance Raman (514.5 nm)

band	I_{rel}	$\lvert\Delta a\rvert$, Å	χ_i', cm^{-1}	assignment
2118	11	0.046	920	ν_{C-N} bridge
2077	3.0	0.012	250	ν_{C-N} term
565	1.9	0.035[a]	580	ν_{M-C} term[b]
539	2.1	0.078[a]	660	ν_{M-C} bridge[b]
492	1	0.039	350	ν_{M-NH_3}
470	0.54	0.061	190	ν_{M-NH_3} (axial)
355	0.36	0.061	170	ν_{M-NC}
270	1.4		860	$\delta_{H_3N-M-NH_3}$

[a] Based on exclusive M–C stretching character in the normal coordinate distortion. (Intervalence enhancement of these bands does suggest an increased M–C stretching character for the unsymmetrical dimer over that found in the monomer.) [b] And δ_{M-CN}.

(42) Volger, A.; Kisslinger, J. *J. Am. Chem. Soc.* **1982**, *104*, 2311.
(43) (a) Nakagawa, I.; Shimanouchi, T. *Spectrochim. Acta* **1962**, *18*, 101. (b) Griffith, W. P.; Turner, G. T. *J. Chem. Soc. A* **1970**, 858. (c) Hawkins, N. J.; Mattraw, H. C.; Sabol, W. W.; Carpenter, D. R. *J. Chem. Phys.* **1955**, *23*, 2422.
(44) Bridging occurs via electron withdrawal from the lowest CN σ^* orbital, effectively increasing the CN bond order and stretching frequency. See, for example: (a) Shriver, D. F.; Shriver, S. A.; Anderson, S. E. *Inorg. Chem.* **1965**, *4*, 725. (b) Hester, R. E.; Nour, E. M. *J. Chem. Soc., Dalton Trans.* **1981**, 939. (c) Allen, C. S.; Van Duyne, R. P. *J. Am. Chem. Soc.* **1981**, *103*, 7497.
(45) Jones, L. H.; Memering, M. N.; Swanson, B. I. *J. Chem. Phys.* **1971**, *54*, 4666.
(46) Electron withdrawal to form the bridging bond presumably reduces the ability to σ bond through the carbon atom, thereby resulting in a decreased force constant for the vibration.
(47) Swanson, B. I.; Hamburg, S. I.; Ryan, R. R. *Inorg. Chem.* **1974**, *13*, 1685.

pletely to bond compression. (3) Again for $Fe(CN)_6^{3-/4-}$, Δa_{CN} is 0.01 ± 0.01 Å[47] versus 0.012 Å for 1. It is worth noting that the C≡N distortion occurs at the limit of precision in the X-ray measurements[47] but that it is rather easily detected and quantitated by postresonance Raman measurements. We have remarked elsewhere, however, that the Raman-based Δa values could be in error by as much as +20% due to spin–orbit coupling and solvent contributions to σ^2 in eq 3.[18]

From the normal coordinate or bond distortion data, individual contributions (χ_i'; Table III) to the vibrational reorganization energy can be calculated:

$$\chi_i' = \tfrac{1}{2}b(\Delta a)^2 f = \tfrac{1}{2}\Delta^2 \nu \qquad (13)$$

From Table III, the following points are worth noting: (1) Both ends of the mixed-valence ion participate in vibrational trapping. (2) Nearly half of the trapping or reorganization energy comes from modes assigned to the bridging ligand. (3) Local modes remote from the metal center (i.e., C≡N stretches) can contribute measurably to the Franck–Condon energy. (4) The low-energy metal–ammine bend (which is generally overlooked) is as significant as the higher energy Ru–NH_3 stretch.

Point 2 has obvious implications with regard to ligand-bridged electrode reactions. For example, it is possible that these reactions will be *decatalyzed* by the creation of additional barrier effects due to surface-to-bridge bond formation. It is interesting to note that Raman studies of $Ru(CN)_6^{4-}$ adsorbed at roughened silver[44c] reveal vibrational energy shifts (C≡N) that are similar in magnitude to those described here for binuclear complex formation.

At this point, it is reasonable to ask whether the Raman analysis can be applied to systems of more direct relevance to electrode reactions. The answer is a tentative "yes". Detectable intervalence transitions exist not only for ligand-bridged dimers but also for assemblies based on simple ion pairing:[50]

$$Ru^{III}(NH_3)_6^{3+}, Ru^{II}(CN)_6^{4-} \xrightarrow{h\nu} Ru^{II}(NH_3)_6^{2+}, Ru^{III}(CN)_6^{3-} \qquad (14)$$

In these outer-sphere systems, the bond length changes from optical excitation are precisely those occurring in the corresponding outer-sphere electrochemical reactions.

We have very recently completed preliminary Raman studies for the system in eq 14 and also for the ferrocyanide/methylviologen ion pair.[51] In both cases, intervalence enhancement exists, and for the $Ru(NH_3)_6^{3+}$, $Ru(CN)_6^{4-}$ combination the pattern of vibrational scattering is similar (apart from bridging-mode enhancement) to that for $(NH_3)_5Ru$–NC–$Ru(CN)_5^-$. Further analysis and details will be given in another report.

One other issue that can be addressed in a very elegant way by resonance Raman spectroscopy is the question of external effects upon internal modes. In particular, there has been extensive speculation regarding specific ligand–solvent (hydrogen bond) interactions and whether these interactions might be strong enough to change force constants and bond lengths within redox-active molecules.[12]

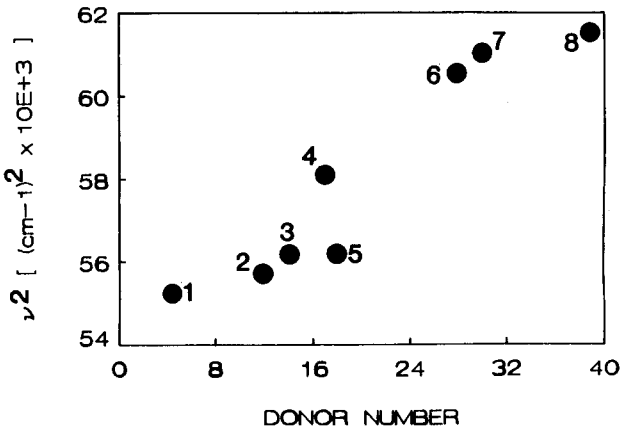

Figure 10. Force constant (as measured by ν^2) for δ (H_3N–Ru–NH_3) as a function of solvent basicity (donor number) in (1) nitrobenzene, (2) benzonitrile, (3) acetonitrile, (4) acetone, (5) H_2O, (6) dimethylacetamide, (7) dimethyl sulfoxide, and (8) hexamethylphosphoramide.

If this were to occur, then there would be obvious implications with regard to solvent and environmental effects upon rates of electrode reactions involving such molecules.

A favorite set of molecules for such speculation has been ammine complexes of ruthenium and cobalt. With that in mind, we chose to examine one particular complex: $(NH_3)_4Ru(bpy)^{2+}$ (bpy = 2,2′-bipyridine).[18] Laser excitation in resonance with the Ru-to-bipyridine charge-transfer band leads to enhanced scattering for 14 modes. Of those many modes, three (an internal bpy mode, the Ru–NH_3 stretch, and an H_3N–Ru–NH_3 bend) display a measurable dependence on the nature of the external solvent. Figure 10 shows that ω^2 (proportional to f) for the H_3N–Ru–NH_3 bend can be correlated with the Lewis basicity of the solvent as measured empirically on Gutman's donor number scale.[52] Such a correlation would be expected if there is specific binding to acidic, coordinated ammines. Mixed-solvent/selective-solvation experiments are consistent with this notion and confirm the local-binding nature of the environmental perturbations.

The conclusions and implications are the following: (1) Force constants for redox relevant, internal modes (e.g., those required for $(NH_3)_4Ru(bpy)^{3+/2+}$ self-exchange or electrochemical exchange) can, indeed, be tuned to a measurable extent by external perturbations. (2) In this system, however, the effects are small. For the available collection of solvents, f changes by ca. 9% for the metal–ammine stretch, 11% for the bend, and just 1% for the bipyridine mode. (3) Because the bond length changes accompanying the oxidation of $(NH_3)_4Ru(bpy)^{2+}$ are also small, the overall rate effects from solvent-induced changes in ΔG_i^* are anticipated to be immeasurably small.

Environmental Factors: Ion Pairing and Ligand Protonation. One of the special characteristics of electron transfer between covalently linked donors and acceptors is the absence of electrostatic work terms (i.e., diffuse double-layer effects at electrodes or Debye–Hückel effects in solution). This special feature permits other environmental effects, especially other electrolyte effects, to be evaluated without undue complication. We[53] (and others[54])

(48) The Raman scattering technique indicates the magnitude, but not the sign, of the distortion. See, however: Myers, A. B.; Mathies, R. A. In *Biological Applications of Raman Spectroscopy*; Spiro, T. G., Ed.; Wiley: New York, Vol. 2.

(49) The comparison to $Fe(CN)_6^{3-/4-}$ may be less than completely appropriate since the extent of back-bonding certainly will differ for M = Ru vs M = Fe. Unfortunately, independent structural data for $Ru(CN)_6^{3-/4-}$ are lacking.

(50) Curtis, J. C.; Meyer, T. J. *Inorg. Chem.* **1982**, *21*, 1562.

(51) Blackbourn, R. L., unpublished experiments.

(52) Gutman, V. *Electrochim. Acta* **1976**, *21*, 661.

(53) (a) Blackbourn, R. L.; Hupp, J. T. *Chem. Phys. Lett.* **1988**, *150*, 399. (b) Blackbourn, R. L.; Dong, Y., unpublished experiments.

(54) (a) Hammack, W. S.; Drickamer, H. G.; Lowery, M. D.; Hendrickson, D. N. *Chem. Phys. Lett.* **1986**, *132*, 231. (b) Lowery, M. D.; Hammack, W. S.; Drickamer, H. G.; Hendrickson, D. N. *J. Am. Chem. Soc.* **1987**, *109*, 8019. (c) Lewis, N. A.; Yaw, O. *J. Am. Chem. Soc.* **1988**, *110*, 2307.

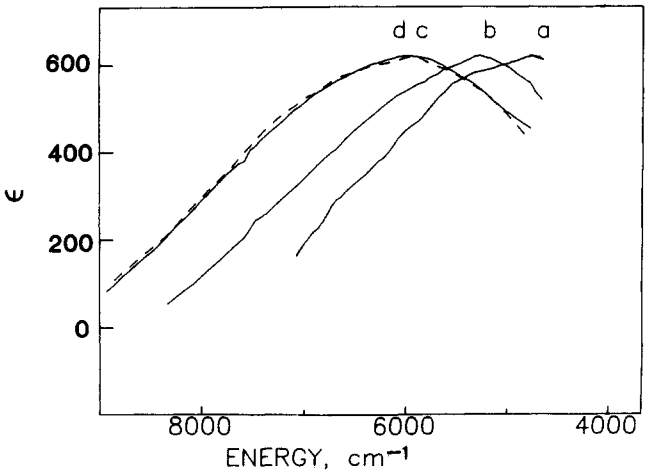

Figure 11. Intervalence absorption bands for (a) 0.008 mM Bf^+, (b) 0.076 mM Bf^+, (c) 3.8 mM Bf^+, and (d) 0.076 mM Bf^+ + 3.1 mM tetrabutylammonium hexafluorophosphate (dashed line); each in CD_2Cl_2 as solvent.

have taken advantage of this circumstance to examine specifically the role of ion pairing in electron-transfer reactions.

Perhaps the simplest and most illustrative case we have examined is optical electron transfer in the acetylene-bridged biferrocene monocation (Fc—C≡C—Fc^+; Bf^+).[53a] Depending on either the chromophore or external electrolyte concentration (or both), either of two intervalence reactions can happen:

$$Fc—C{\equiv}C—Fc^+ \xrightarrow{h\nu} {}^+Fc—C{\equiv}C—Fc^* \quad (15a)$$

$$Fc—C{\equiv}C—Fc^+,X^- \xrightarrow{h\nu} {}^+Fc—C{\equiv}C—Fc,X^{-*} \quad (15b)$$

With methylene chloride as the solvent and PF_6^- as the counterion, the ion-pairing constant (K_{IP}) is such that the first pathway dominates at micromolar concentrations; the second one dominates at millimolar concentrations. At even higher concentrations, a third pathway, evidently involving ion-pair aggregation, intervenes.

Figure 11 illustrates the effects of ion pairing (and higher order association) upon the absorption band for the intervalence transition. The main finding is that the optical barrier moves to substantially higher energy (ΔE_{op} = 1560 cm^{-1} or 4.4 kcal mol^{-1}, for 3.8 mM Bf^+ vs 0.008 mM Bf^+).

Bandwidth studies rule out the possibility of a change in reorganization energy. The change in E_{op} comes instead from ion-pairing-induced redox asymmetry. In other words, eq 15b occurs in an "uphill" sense thermodynamically, even though the overall reaction (ET followed by counterion migration) must occur without a change in free energy (because of chemical symmetry). As indicated in Figure 12, the extent of redox asymmetry is given by RT ln K_{IP}/K_{IP}^* where K_{IP}^* is the equilibrium constant for pairing to the neutral end of $^+$Fc—C≡C—Fc.

A very similar circumstance will exist for thermally activated ET. Here a two-step reaction can be written:

$$Fc—C{\equiv}C—Fc^+,X^- \xrightarrow{E} {}^+Fc—C{\equiv}C—Fc,X^- \quad (16)$$

$$^+Fc—C{\equiv}C—Fc,X^- \xrightarrow{C} X^-,{}^+Fc—C{\equiv}C—Fc \quad (17)$$

The sequence should be recognizable as a very simple intramolecular EC scheme. If the E step is rate determining, then (from Figure 12) the activation free energy will increase with ion pairing by roughly 0.5 RT ln K_{IP}/K_{IP}^*. Consequently, a rate decrease should occur upon ion pairing. There are, in fact, a number of examples of this effect for *bimolecular* systems,[55-60] and we have recently reviewed these in the context of optical intervalence experiments.[61]

The important point for interfacial reactions is that these also can involve coupled ion motion:

$$Fc^+,X^- + e^- \xrightarrow{E} Fc,X^- \quad (18)$$

$$Fc,X^- \xrightarrow{C} Fc + X^- \quad (19)$$

The reaction in eq 18 again is uphill by $\Delta E = RT$ ln $K_{IP}(Fc^+)/K_{IP}(Fc)$, and the activation barrier should be affected to the extent of $\sim 0.5\Delta E$.[62] If the mixed-valence reaction in eq 15 is a suitable model for the electrochemical barrier energetics, then the predicted effect from optical studies of ion tripling[53a] or ion-pair aggregation (methylene chloride as solvent) is a 50-fold decrease in standard rate constant.

Our studies in more polar solvents suggest that the rate effects will be smaller in those cases.[61] (For example, a rate decrease of 2.8 is predicted for acetonitrile.[61]) The effects can also vary with the nature of the counterion. For example, optical experiments in water with

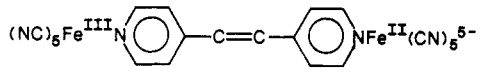

show progressively larger barrier effects for Li^+ vs Ca^{2+} vs La^{3+} as the electrolyte cation.[63]

A closely related class of reactions are those based on redox protonation (e.g., quinone/hydroquinone, ferricyanide/ferrocyanide in acid, etc.). When these are configured as optical reactions, there is an opportunity to measure directly the effect of proton demand upon the charge-transfer barrier. As an example, we have examined optically the first step of the following intramolecular "EC" reaction:[53b]

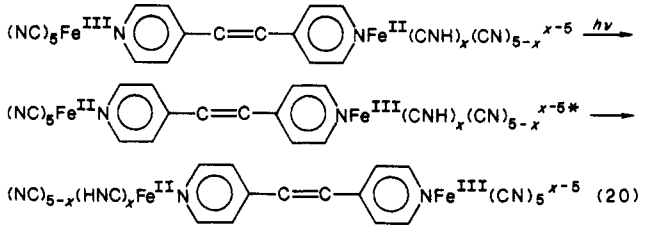

(55) Excluded from ref 56–60 are trivial examples where both reactants carry charges and the charges are of opposite sign. There, ion pairing between one reactant and an electrolyte component will lead to a decrease in the electron-transfer rate simply because of a decrease in the precursor complex stability constant.

(56) (a) Borchardt, D.; Wherland, S. *Inorg. Chem.* **1984**, *23*, 2537. (b) Borchardt, D.; Pool, K.; Wherland, S. *Inorg. Chem.* **1981**, *21*, 93.

(57) (a) Yang, E. S.; Chan, M.-S.; Wahl, A. C. *J. Phys. Chem.* **1975**, *79*, 2049; **1980**, *84*, 3094. (b) Nielson, R. M.; McManis, G. E.; Safford, L. K.; Weaver, M. J. *J. Phys. Chem.*, in print.

(58) Li, T. T.-T.; Weaver, M. J.; Brubaker, C. H. *J. Am. Chem. Soc.* **1982**, *104*, 2381.

(59) (a) Zandstra, P. J.; Weissman, S. I. *J. Am. Chem. Soc.* **1962**, *84*, 4269. (b) Hirota, N.; Carraway, R.; Schook, W. *J. Am. Chem. Soc.* **1968**, *90*, 3611. (c) Höfelmann, K.; Jagur-Grodzinski, J.; Szwarc, M. *J. Am. Chem. Soc.* **1969**, *91*, 4645. (d) Suga, K.; Aoyagui, S. *Bull. Chem. Soc. Jpn.* **1982**, *55*, 358. (e) Chang, R.; Johnson, C. S. *J. Am. Chem. Soc.* **1966**, *88*, 2338.

(60) (a) Szwarc, M. *Acc. Chem. Res.* **1972**, *5*, 169. (b) Szwarc, M. *Ions and Ion Pairs in Organic Reactions*; Wiley: New York, 1975; Vol. 2, Chapter 1 and references therein.

(61) Blackbourn, R. L.; Hupp, J. T., manuscript in preparation.

(62) For a different perspective, but a similar conclusion, see: Fawcett, W. R.; Laisa, A. *J. Phys. Chem.* **1978**, *94*, 237.

(63) Dong, Y.; Blackbourn, R. L.; Zhang, H. T., unpublished experiments.

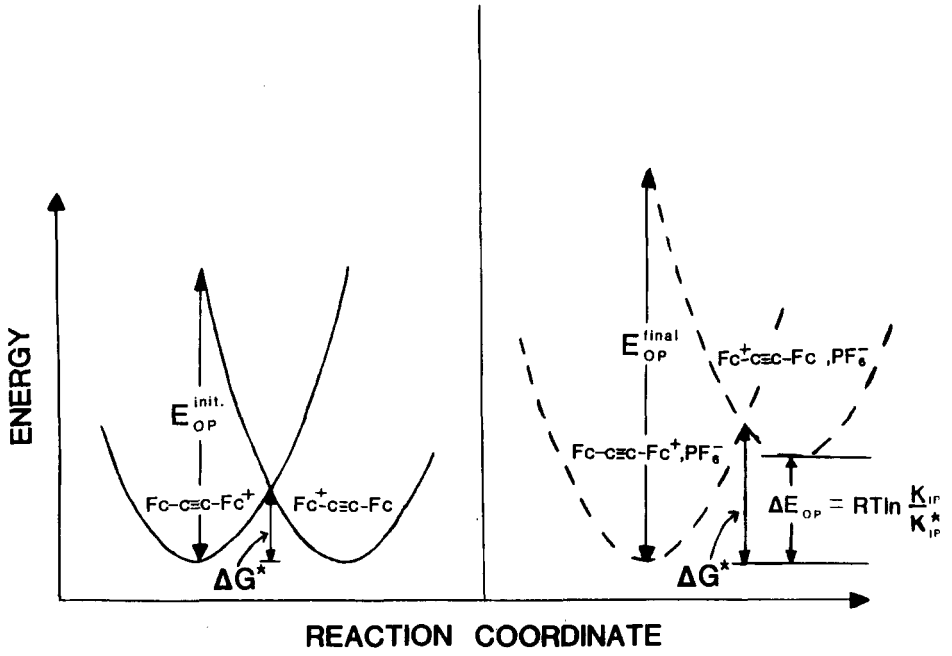

Figure 12. Schematic representation of zero-order potential energy surfaces for various acetylene-bridged biferrocene mixed-valence species.

Protonation begins at about pH 4.5, and, in principle, up to five protons can be added in highly acidic solutions. Consequently, below pH 4.5, E_{op} begins to shift higher in energy. Ultimately, the energy effects are enormous; in 2 M HCl, E_{op} is more than 5000 cm^{-1} larger than in neutral solution.

Despite their large size, effects of this magnitude ought not to be surprising. Similarly, enormous *rate* effects from proton demand are known for certain electrode reactions.[64] The real value of the optical experiments in electrode kinetics may come from the eventual ability to separate thermodynamic protonation effects from the vibrational protonation effects (i.e., pH-induced force constant and bond length alterations). Indeed, our current efforts are focused in that direction.

Electronic Coupling. Intervalence absorption measurements provide an excellent quantitative means of assessing electronic coupling between spatially isolated donor and acceptor orbitals. Richardson and Taube, in particular, have recognized this point.[25] Along with others,[17] they have investigated how coupling depends on separation distance, bridge conjugation, orbital symmetry, and so on.

We want to show here how another issue—the driving-force dependence—can be investigated through optical experimentation. The specific system is the one shown in eq 15:

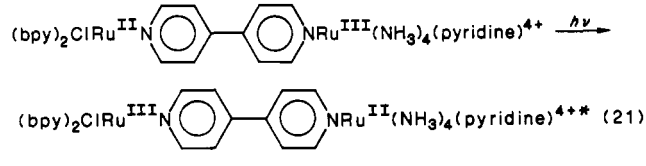

To a good approximation (i.e., a few tens of millivolts or less), the driving force for eq 21 can be evaluated simply from the difference in formal potential (E_f) for the two ends. Because E_f for the tetraammine end (only) depends strongly on solvent, it is possible to obtain a range of driving forces simply by performing the optical experiment in a suitable range of solvents.

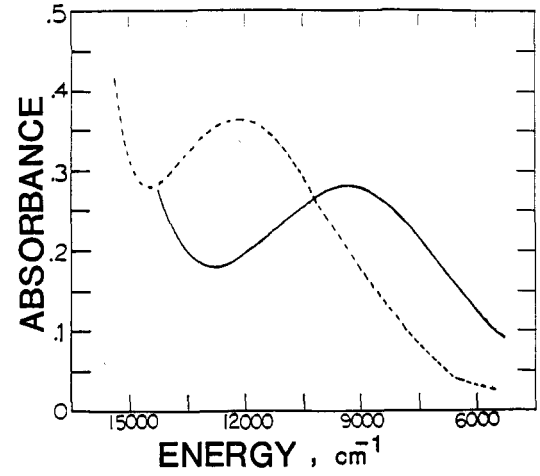

Figure 13. Intervalence absorption bands for (bpy)$_2$ClRu-4,4′-bpy-Ru(NH$_3$)$_4$(pyridine)$^{4+}$ in nitrobenzene (solid line) and propylene carbonate (dashed line). Concentration = 0.86 mM; path length = 1 cm.

Figure 13 shows some representative results. The intervalence absorption band obtained in propylene carbonate (ΔE = 0.296 V) differs both in energy and intensity from that in nitrobenzene (ΔE = 0.119 V). The energy effect is easily understandable in terms of eq 5. The intensity effect is a bit more subtle. For an electronic transition, the integrated absorption intensity will tell us something about how "allowed", in a spectroscopic sense, the transition is; qualitatively, at least, the optical reaction appears to be more highly allowed in propylene carbonate as solvent. This in turn suggests greater initial state/final state coupling.

To quantitate our observations, we turn to perturbation theory. From Mulliken's treatment of donor–acceptor mixing[65] we obtain for the square of the bridged-mediated interaction energy[25]

$$\bar{H}_{13}^2 = (4.24 \times 10^{-4})\epsilon_{max}\Delta\bar{\nu}_{1/2}E_{op}/d^2 \qquad (22)$$

(64) For example: Vetter, K. J. *Z. Elektrochem.* **1952**, *56*, 797.

(65) Mulliken, R. S.; Person, W. B. *Molecular Complexes*; Wiley: New York, 1969.

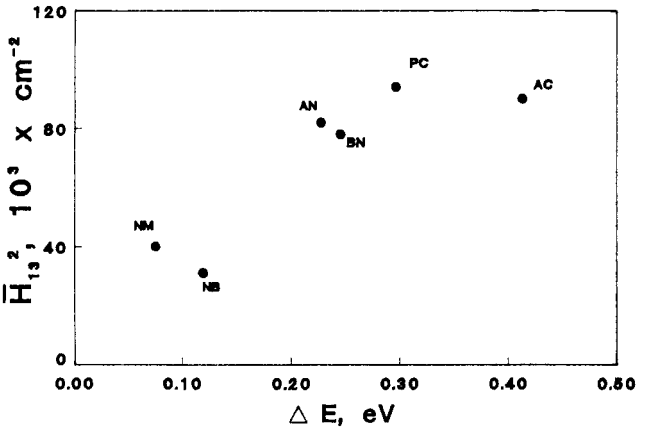

Figure 14. Dependence of $\bar{H}_{13}^2$ on redox asymmetry for $(bpy)_2ClRu$–4,4′-bpy–$Ru(NH_3)_4$(pyridine)$^{4+}$. ΔE was estimated electrochemically. (For nitromethane as solvent, ΔE was estimated from measurments on an Os–Ru analogue). Key to solvents: NM, nitromethane; NB, nitrobenzene; BN, benzonitrile; PC, propylene carbonate; AN, acetonitrile; AC, acetone.

In eq 22, ϵ_{max} is the extinction coefficient of the intervalence absorption band at E_{op}, $\Delta\bar{\nu}_{1/2}$ is its width at half-height, and the other terms have been defined previously.

Analysis of our data for reaction 21 leads to the plot in Figure 14. The key observation is that $\bar{H}_{13}^2$ (and therefore the degree of electronic adiabaticity) increases detectably with increasing ΔE (i.e., with increasingly unfavorable driving force). The result, in fact, is consistent (at least in a general sense) with expectations from various superexchange treatments of mediated donor–acceptor interactions;[25,66] the exact details are the focus of ongoing experimental inquiries. For electrochemical processes, however, the implication seems clear: electronic coupling at the interface should depend on the reaction driving force or overpotential.[67]

(66) (a) Beratan, D. N.; Hopfield, J. J. *J. Am. Chem. Soc.* **1984**, *106*, 1584. (b) McConnell, H. M. *J. Chem. Phys.* **1961**, *35*, 508. (c) Marcus, R. A. *Chem. Phys. Lett.* **1987**, *133*, 471; **1988**, *146*, 13.

(67) An alternative or additional implication is that coupling at the interface will depend on the nature of the solvent. We have insufficient optical information at present to distinguish between these two explanations or predictions.

(68) EC is a well-established mechanistic shorthand notation for an interfacial electron-transfer step followed by a purely chemical step.

Summary

A number of ingredients are known or thought to be important in determining rates of electrochemical reactions and, therefore, mechanisms of electrocatalysis. These ingredients may include bond reorganization, solvent reorganization, electronic coupling, ion pairing, proton demand, "work terms", and free-energy driving-force effects. Although evidence exists, in general, for a detectable role for each one of these, for specific cases there is often uncertainty about the relative importance of each individual effect. Kinetic studies alone do not always provide a sufficient basis for resolving the problem. On the other hand, when appropriately utilized, optical electron-transfer measurements do provide an unambiguous way of accurately partitioning rates into their component effects. Furthermore, the partitioning is achieved in a way that is largely independent of modelistic assumptions.

Initial attempts to apply optical intervalence methods to problems of electrochemical interest suggest, first, that single-electron-transfer reactions can be handled quite elegantly and, second, that simple EC reactions are also amenable to detailed investigation. Some of the more interesting possibilities have been illustrated by case studies of solvent reorganization, bond reorganization, ion-pairing effects, proton demand, and electronic coupling. Other possibilities undoubtedly exist. In our view, the most significant challenges for the future will be (1) the continued development of techniques that are fully appropriate for redox *monomers* (cf., preliminary Raman studies, above) and (2) extension of the approach to *multi*electron-transfer reactions. Both are points of focus for ongoing research in our laboratory.

Acknowledgment. Our work on optical electron-transfer reactions and electrode kinetics has been supported by the Department of Energy, Office of Energy Research, Division of Chemical Sciences (Grant No. DEFG02-87ER13808); the Office of Naval Research; and the donors of the Petroleum Research Fund, administered by the American Chemical Society. Matching support from NSF has been provided by a Presidential Young Investigator Award (CHE-8552627). The Raman facilities are part of the Materials Research Center at Northwestern (NSF-DMR-8520280).